7-1-2020

A novel, reliable protocol to objectively assess scar stiffness using shear wave elastography

Helen DeJong
Edith Cowan University

Steven Abbott

Marilyn Zelesco

Katrina Spilsbury

Lisa Martin

See next page for additional authors

10.1016/j.ultrasmedbio.2020.03.003
DeJong, H., Abbott, S., Zelesco, M., Spilsbury, K., Martin, L., Sanderson, R., ... & Wood, F. M. (2020). A Novel, Reliable Protocol to Objectively Assess Scar Stiffness Using Shear Wave Elastography. Ultrasound in Medicine & Biology, 46(7) 1614 - 1629. https://doi.org/10.1016/j.ultrasmedbio.2020.03.003

Ultrasound in Med. & Biol., Vol. 46, No. 7, pp. 1614–1629, 2020

0301-5629/$ - see front matter

https://doi.org/10.1016/j.ultrasmedbio.2020.03.003

● *Original Contribution*

A NOVEL, RELIABLE PROTOCOL TO OBJECTIVELY ASSESS SCAR STIFFNESS USING SHEAR WAVE ELASTOGRAPHY

HELEN DEJONG,[*,†,‡,§] STEVEN ABBOTT,[¶] MARILYN ZELESCO,[¶] KATRINA SPILSBURY,[‖] LISA MARTIN,[§,#] ROWAN SANDERSON,[‡,**] MELANIE ZIMAN,[†,††] BRENDAN F. KENNEDY,[‡,**] and FIONA M. WOOD[§,#,‡‡]

* Perth Scar and Pain Clinic, Fremantle, Western Australia 6160, Australia; † School of Medical and Health Science, Edith Cowan University, Joondalup, Western Australia 6027, Australia; ‡ BRITElab, Harry Perkins Institute of Medical Research, QEII Medical Centre Nedlands and Centre for Medical Research, University of Western Australia, Crawley, Western Australia 6009, Australia; § Fiona Wood Foundation, Fiona Stanley Hospital, Murdoch, Western Australia 6150, Australia; ¶ Department of Medical Imaging, Fiona Stanley Hospital, Murdoch, Western Australia 6150, Australia; ‖ Institute for Health Research, University of Notre Dame Australia, Fremantle, Western Australia 6959, Australia; # Burn Injury Research Unit, University of Western Australia, Crawley, Western Australia 6009, Australia; ** Department of Electrical, Electronic and Computer Engineering, School of Engineering, University of Western Australia, Crawley 6009, Western Australia; †† School of Biomedical Science, University of Western Australia, Crawley, Western Australia 6009, Australia; and ‡‡ Burn Service of Western Australia, Fiona Stanley Hospital, Murdoch, Western Australia 6150, Australia

(*Received* 16 *June* 2019; *revised* 28 *February* 2020; *in final from* 6 *March* 2020)

Abstract—The aim of this research was to investigate the use of shear wave elastography as a novel tool to quantify and visualize scar stiffness after a burn. Increased scar stiffness is indicative of pathologic scarring which is associated with persistent pain, chronic itch and restricted range of movement. Fifty-five participants with a total of 96 scars and 69 contralateral normal skin sites were evaluated. A unique protocol was developed to enable imaging of the raised and uneven burn scars. Intra-rater and inter-rater reliability was excellent (intra-class correlation coefficient >0.97), and test–retest reliability was good (intra-class correlation coefficient >0.85). Shear wave elastography was able to differentiate between normal skin, pathologic scars and non-pathologic scars, with preliminary cutoff values identified. Significant correlations were found between shear wave velocity and subjective clinical scar assessment ($r = 0.66$). Shear wave elastography was able to provide unique information associated with pathologic scarring and shows promise as a clinical assessment and research tool. (E-mail: info@perthspc.com.au)

Key Words: **Elastography, Shear wave elastography, 2-D shear wave elastography, Objective scar assessment, Burn, Scar pliability, Reliability.**

INTRODUCTION

Scars form as part of the healing process after injury, surgery or disease (Ferguson and O'Kane 2004). Compared with normal tissue, scars can develop increased stiffness and thickness and reduced extensibility, which are often associated with chronic pain (Browne et al. 2011), psychological distress and movement restrictions (DeJong et al. 2017b). Scars are also associated with an increased risk of cancer (Duke et al. 2012, 2014; Kallini et al. 2015), organ dysregulation (Hinz 2015) and a wide range of systemic complications (Fear and Wood 2018; Barrett et al. 2019). Historically, increased scar stiffness was considered to be an end product of overzealous wound healing (Ferguson and O'Kane 2004). However, it is now recognized that increased scar stiffness is a dynamic component of a self-perpetuating fibrotic cycle underpinning pathologic scar formation (Hinz 2015). This cycle begins early in wound healing, long before it is clinically palpable, and can remain active for many years after injury. Various therapies can modify the process, with early interventions considered more effective than the treatment of mature scars (Ferguson and O'Kane 2004; Walraven and Hinz 2018). Current tools for clinical assessment of scar stiffness are inadequate and rely on

Address correspondence to: Helen DeJong, School of Medical and Health Science, Edith Cowan University, 8a Milne Street Bicton, Western Australia 6157. Australia. E-mail: info@perthspc.com.au

subjective palpation. Therefore, a method for quantifying scar stiffness is required to help identify pre-clinical scar stiffness so targeted early interventions can be initiated and treatment effects evaluated. Furthermore, objective clinical assessment tools are required to investigate the relationship between scar stiffness and the pathologic pathways associated with fibrosis so novel treatments can be developed to improve scar outcome.

Ultrasound imaging is a reliable method of evaluating the structural architecture of the skin in a range of cutaneous conditions including burns (Wang et al. 2010; Li et al. 2013; Simons et al. 2017), systemic sclerosis (Hesselstrand et al. 2008; Santiago et al. 2016) and skin cancer (Mandava et al. 2013; Wortsman 2018). Ultrasound is clinically accessible, relatively low cost, tolerable and, with appropriate training, easy to use. An adjunct to standard B-mode ultrasound is elastography, which measures the mechanical properties of tissues (Bamber et al. 2013; Dietrich et al. 2017) and provides color-coded images (elastogram) to visualize tissue stiffness in depth sections. Developed in the 1990s (Ophir et al. 1991; Sarvazyan et al. 1998), elastography has been widely used to image liver (Ferraioli et al. 2015), breast (Barr et al. 2015) and musculoskeletal disorders (Creze et al. 2018); however, it is relatively new to dermatology.

An initial study evaluating two keloid (raised, pathologic) scars revealed differences in stiffness between the immature and mature scars (Aya et al. 2014). A method known as strain elastography, in which the operator applies a manual compression force on the tissues with a probe, was used (DeJong et al. 2017a). This method is user dependent and provides a qualitative method of assessment (Bamber et al. 2013). A later study by the same group using shear wave elastography (SWE) presented three case studies illustrating correlations between the elastogram and histology of keloid scars (Aya et al. 2015). The main difference in the technology is that SWE uses an acoustic radiation force (ARF) generated from within the ultrasound transducer itself, rather than a force generated manually by the operator. The tissue displacement from the ARF generates shear waves that propagate away from the force and are tracked by multiple imaging beams, providing a measurement of shear wave speed (SWS), which is less user dependent (Lee et al. 2015). SWE has also been used to evaluate skin stiffness associated with systemic sclerosis (Lee et al. 2015; Santiago et al. 2016; Wang et al. 2017; Yang et al. 2019) and normal skin (Yang et al. 2018).

Previous reliability studies using SWE in skin and skin conditions have been variable, exhibiting moderate to excellent reliability in normal skin (Sun et al. 2017; Xiang et al. 2017) and poor to excellent reliability in evaluation of systemic sclerosis (Santiago et al. 2016). SWE reliability in superficial tissues may be influenced by transducer pressure on the skin, which can cause localized pre-stress and high artifactual SWS (Bamber et al. 2013; Săftoiu et al. 2019). "Copious amounts of gel" have been used to minimize this risk (Liu et al. 2015; Botar-Jid et al. 2016; Santiago et al. 2016; Wang et al. 2017; Yang et al. 2018, 2019); however, this may affect the depth of the B-mode focal zone within the displayed field of view. The depth of the focal zone has been reported to influence SWS (Chang et al. 2013; Shin et al. 2016; Palmeri et al. 2017). Semisolid standoffs, ranging in thickness from 2−10 mm, have also been used in cutaneous elastography (Cannaò et al. 2014; Morris et al. 2018). This allows the operator to place the SWE elastogram over the most superfical component of the area of interest.

The main aim of this research was to evaluate the use of SWE as a novel tool to evaluate burn scars in adults. However, scars raised above the surface of the skin provide an additional challenge to obtaining quality images. Imaging uneven skin surfaces has been found to generate large acoustic reflections, wave distortions (Hu et al. 2018) and spurious stiffness (Bhatia et al. 2012a, 2012b). Furthermore, small changes in probe position, or "probe drift," will create variable measurements in repeat images because of scar variability (Nedelec et al. 2008). As a result of these imaging challenges, a novel standoff was developed to acquire elastograms of burn scars. Therefore, reliability for the novel standoff was evaluated first, and then the use of SWE to discriminate between normal skin, non-pathologic scars and pathologic scars was evaluated

METHODS

A cross-sectional pilot study was designed to evaluate both the reliability and ability of SWE to discriminate between skin and scars. The study was approved by the South Metropolitan Health Services Ethics Committee (EC00265) in Western Australia.

Participants were recruited from the Burns Outpatient Clinic at Fiona Stanley Hospital, Perth, Western Australia. Participants aged ≥18 y with at least one scar undergoing active treatment were invited to participate. Participants were excluded if they were being treated for open wounds, were not able to provide written consent because of psychological, cognitive or language barriers or had a pre-existing dermatologic condition, (*e.g.,* dermatitis, eczema and psoriasis). In addition, participants were excluded if they were less than 6 wk post-injury or less than 6 wk post-secondary surgical intervention, (*e.g.,* laser, z-plasty or steroid injection).

Personnel

Three raters were involved in this study. Rater 1 (H.D.) was a senior occupational therapist with more than 20 y of experience in the assessment and treatment of scars, but was a novice to SWE. Rater 1 received approximately 10 h of training in the use of SWE by raters 2 and 3. Subjective scar assessments were conducted by rater 1 before SWE

assessment. Rater 2 (S.A.) was a senior sonographer with more than 10 y of experience in sonography and 5 y of experience using elastography. Rater 3 (Ma.Z.) was a senior sonographer with more than 31 y of experience in sonography and 11 y of experience using elastography.

Subjective scar assessment

Scars were assessed subjectively using the Vancouver Scar Scale (VSS) (Baryza and Baryza 1995), which is a validated scar assessment tool (Table 1) (Gankande et al. 2013; Thompson et al. 2015). The VSS is used to evaluate four clinical characteristics of scarring: Vascularity, Pigmentation, Pliability and Height (van der Wal et al. 2014). Each scar characteristic is considered independent so only the VSS Height and Pliability scores were evaluated in this study. Some scars after a burn may return to "normal" height and/or stiffness, scoring '0' in either or both of the VSS Height and Pliability categories. Therefore, a VSS score $\geq$1 in either the Height or Pliability category represents clinically detected pathophysiology, with a Height score $\geq$1 indicating a hypertrophic scar (Thompson et al. 2015).

Elastography

An ACUSON S3000 ultrasound system (Siemens Heathineers Pty Ltd, Australia and New Zealand) with a 9 L4 linear transducer was used in this study. In the Virtual Touch IQ elastography mode, a sequence of ARF push pulses ranging from 4.00−5.71 MHz are sent to a specific region of interest (ROI) in the tissue. The push pulses cause tissue displacement on the order of 1−10 μm and generate shear waves that propagate orthogonal to the push pulse. Multiple detection beams follow the push pulses to capture the SWS. A color-coded, static 2-D SWE map (elastogram) is overlaid on the B-mode ultrasound image to visualize tissue stiffness (Fig. 1b), whereby each color pixel represents the estimated SWS at that location. Red pixels represent stiffer regions, and blue pixels represent softer regions. Built-in software provides a quality map ensuring the shear wave was of sufficient magnitude with adequate signal-to-noise ratio. Sampling boxes (1.5 mm^2) are then placed onto the images to obtain a quantitative measurement of SWS (Fig. 1c), reported in meters per second. SWS correlates to tissue stiffness, with higher speeds indicating stiffer tissue. In addition, shear modulus measurements are calculated from the SWS by in-built software, providing an estimate of tissue elasticity reported in kiloPascals. Although well-established principles and equations are used to estimate shear modulus (Lee et al. 2015; Dietrich et al. 2017; O'Hara et al. 2019), the equation relating SWS to shear modulus employs a number of assumptions regarding the tissues, for example, homogeneity, isotropy and pure shear wave propagation, which have not been fully tested on the skin (Bamber et al. 2013; Dietrich et al. 2017). As such, in line with a precedent in the field (Bamber et al. 2013; Lee et al. 2015; Luo et al. 2015), statistical analysis was performed using SWS, as this is the actual measured parameter. The converted shear modulus is still presented in the results for comparative purposes.

Table 1. Modified Vancouver Scar Scale (Baryza and Baryza 1995)

Skin characteristic	Parameter
Pliability	
0	Normal
1	Supple
2	Yielding
3	Firm
4	Banding
5	Contracture
Height	
0	Normal-flat
1	>0 to 1 mm
2	>1 to 2 mm
3	>2 to 4 mm
4	>4 mm
Vascularity	
0	Normal
1	Pink
2	Red
3	Purple
Pigmentation	
0	Normal
1	Hypo-pigmentation
2	Mixed pigmentation
3	Hyper-pigmentation

The novel standoff

A custom-made standoff (Fig. 2) was fabricated to deal with the uneven topography of the scar surface and prevent probe drift. In essence, a semisolid standoff with a central cutout section was developed to contain the transmission gel. The "gel well" was made from a two-part silicone elastomer (Elastosil P7676, Wacker Chemie AG, Germany). The elastomer resin and cross-linker were mixed in equal parts before being poured into a 40 × 20 × 10-mm 3-D printed mold of the gel well. The mold, designed using SolidWorks (Dassault Systèms, France), featured a 30 × 10 × 10-mm cutaway at the center of the gel well, which was used to contain the transmission gel and was designed to fit the base of the 9 L4 probe. An oven was used to cure the silicone in the mold at 70°C for 30 min before the gel well was removed. The gel well had a Young's modulus of 16 kPa and so was compliant enough to conform to the contours of the body. The 10-mm thickness ensured the skin/scar was maintained within the focal zone (Dillman et al. 2015), the axial compression forces from the probe were minimal and good coupling was maintained with the uneven surface of raised scars.

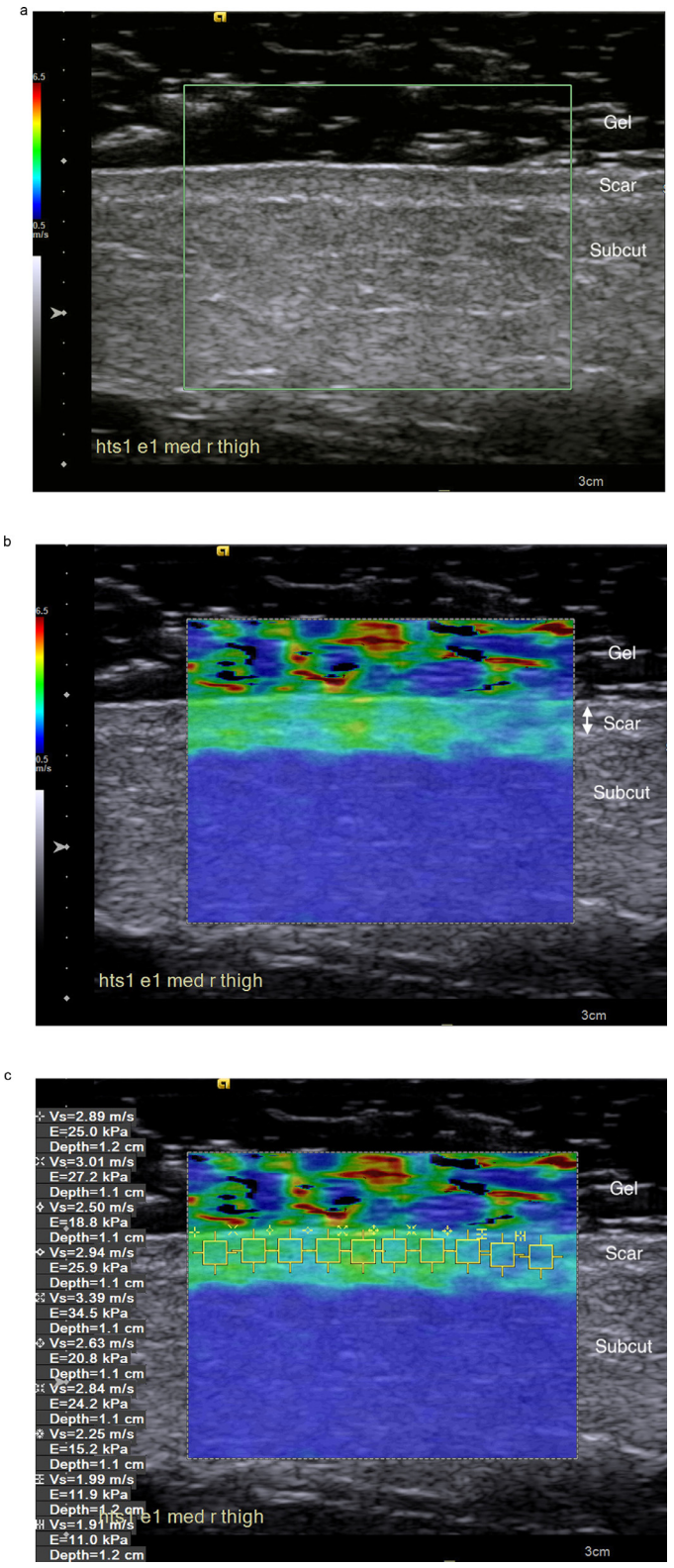

Fig. 1. Shear wave elastography. (a) Ultrasound image of a 12-mo-old scar resulting from a deep partial-thickness flame burn on the thigh of a 57-y-old man. The scar was flat and had a Vancouver Scar Scale Pliability score of 2. (b) Associated elastogram. (c) Associated elastogram with 10 sampling boxes positioned to capture the shear wave speed of the scar.

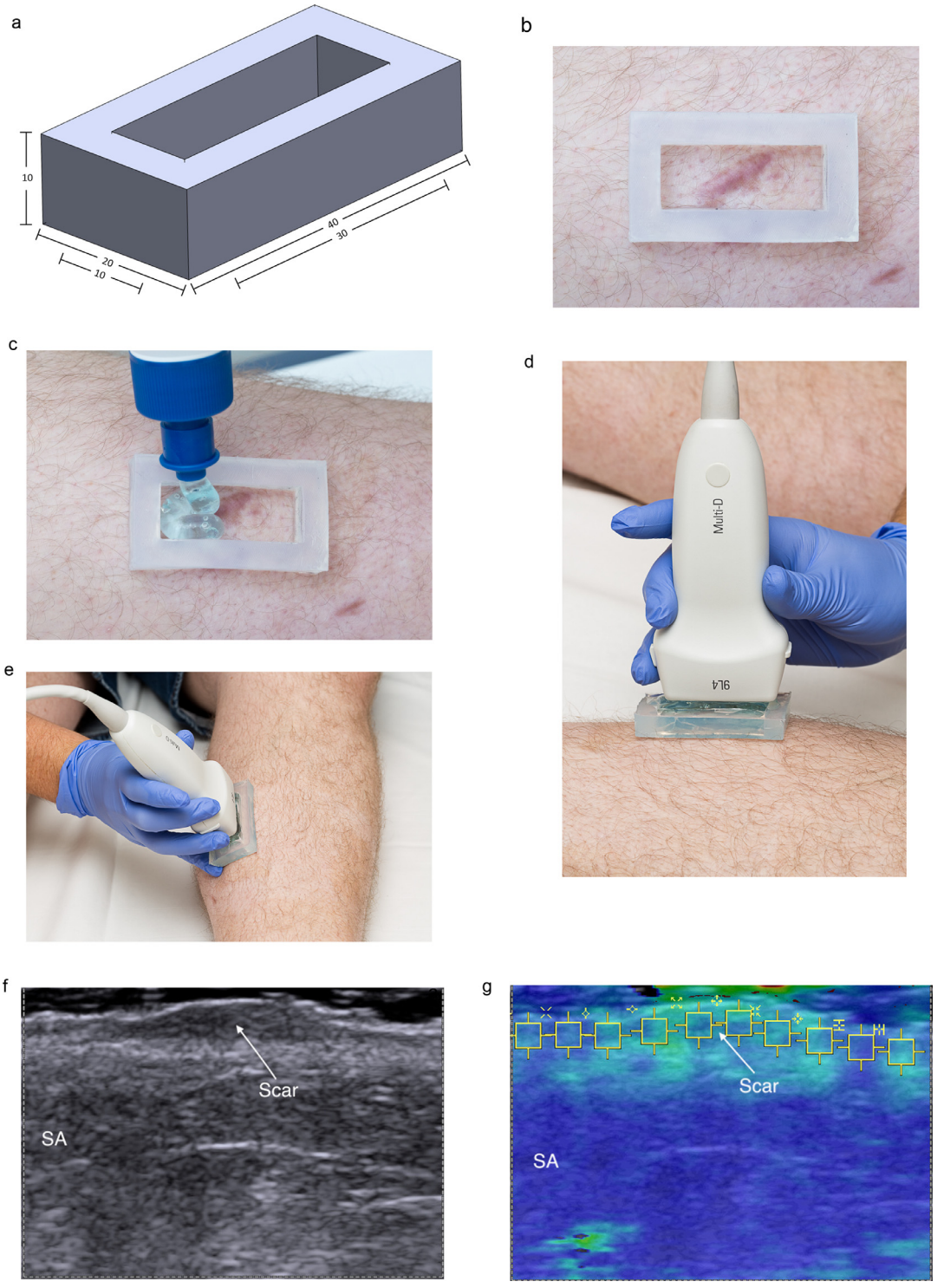

Fig. 2. The novel "gel well" standoff. (a) A diagram outlining the dimensions of the gel well. (b) Image of the silicon gel well placed over a scar. (c) Transmission gel being poured into the centre of the gel well. (d) The ultrasound probe positioned on the gel well, held perpendicular to the scar with minimal pressure. (e) The probe positioned over the scar at a different angle. (f) Resultant ultrasound image. (g) Resultant elastogram. SA = subcutaneous adipose tissue.

Procedure

Participants meeting the inclusion criteria were recruited by rater 1. Informed, written consent was obtained, and scar sites were identified. Up to three discrete scar sites and three contralateral normal skin sites (controls) were evaluated. A previous SWE study had reported that contralateral skin sites are suitable to act as controls for skin conditions, illustrating minimal differences between the two sides (Xiang et al. 2017). In some instances, a control site could not be evaluated because of bilateral burns or previous injury on the contralateral side. The scar sites were 30 × 10 mm, the same size as the skin contact region of the elastography probe. Scar sites were chosen to provide a variety of scar severities, so that the capacity of SWE to evaluate different levels of scarring could be assessed. The VSS was completed for each scar site before both ultrasound and elastography. The participant was positioned on a hospital bed in a temperature-controlled room (22˚C). The body was positioned so the scar was horizontal, and the surrounding joints were placed in a position to minimize tension/stretch on the scar. The position of the control site mirrored the scar position.

The gel well was placed over the scar and filled with transmission gel. The transducer was placed gently on top, held perpendicular to the skin with only minimal pressure applied. The system was switched to elastography mode. The penetration depth was set to 30 mm and the elastography ROI was 20 × 25 mm. The elastography ROI was set to ensure that the epidermis and subcutaneous adipose tissue were both clearly captured. The velocity display scale was set at 0.5 to 6.5 m/s; however, it was adjusted to 10 m/s when tissues were extremely stiff and SWS exceeded 6.5 m/s. This does not alter the SWS, only the visual display.

An ultrasound image was acquired, ensuring a clearly defined entry echo was visible. The sonogram was evaluated for artifact and then archived. The elastogram was then acquired, ensuring the probe was held steady and the participant was relaxed and stable. The elastogram was evaluated for artifact, sampling boxes were inserted and the image was saved. Because the elastograms are not visualized until after acquisition, up to five elastograms were acquired if required, to obtain three elastograms with minimal artifact.

Objective measurement protocol

Manual placement of the sampling boxes within the elastogram was completed by the rater after image acquisition. Initially five boxes were placed underneath the epidermal entry echo, and five boxes directly below within the subcutaneous adipose, to capture objective measurements of both tissues. However, the elastograms of scar tissue revealed a high level of heterogeneity, and therefore, the five measurement boxes could inadvertently be placed to avoid or include stiffer areas. The protocol was adjusted so that the ROI could fit 10 sampling boxes at approximately equal distances from each other, ensuring the horizontal box tails were either touching or were vertically aligned (Fig. 1c). The 10 sampling boxes were placed underneath the epidermal entry echo only, thereby reducing rater bias and capturing the variability of the scar stiffness within the ROI. This change was made before evaluating reliability.

Reliability testing

Intra-rater, inter-rater and test−retest reliability were evaluated. Intra-rater reliability evaluated the consistency among three consecutive images acquired at each site by each rater. Inter-rater reliability evaluated the level of agreement between the two raters whereby rater 2 entered the room after image acquisition by rater 1. The scars were already covered by the gel-filled well; therefore, rater 2 was blinded to the scar underneath. In addition, rater 2 was blind to the elastograms and velocity measurements acquired by rater 1. Rater 2 followed the same imaging protocol as rater 1.

Test−retest reliability evaluated the repeatability of measurements taken by rater 1 at two different time points. At time point 1, before taking any images, rater 1 took a tracing of the scar and the gel well position, noting significant landmarks so the scar could be relocated at time point 2. The assessments at time point 2 were made within 10 d for scars that were more than 3 mo after the injury, and within 5 d for scars less than 3 mo after the injury, to maximize patient participation while minimizing the likelihood of change in scar tissue. At retest, rater 1 was blinded to the images and velocity measurements taken at time point 1.

Statistical analysis

Analysis was completed with Stata Edition 14.0 (StataCorp LP, 2015) using the mean velocity measurements (SWS).

Reliability was tested using the intra-class correlation coefficient (ICC) of the mean SWS. Interpretations of ICC values are summarized in Table 2 (Koo and Li 2016). It is recommended that the ICC should have a value of at least 0.90 for clinical use (Trevethan 2017)

Table 2. ICC interpretation (Koo and Li 2016)

ICC	Reliability
<0.5	Poor
0.5−0.75	Moderate
0.75−0.9	Good
>0.9	Excellent

ICC = intra-class correlation coefficient.

and at least 0.7 for research (Simons et al. 2017). To evaluate intra-rater reliability, ICC estimates and their 95% confidence intervals (CIs) were calculated based on the mean SWS ($k = 3$) using an absolute agreement, two-way mixed effects model. The ICC was calculated using the SWS of all elastograms taken at both time points. To evaluate inter-rater reliability, ICC estimates and their 95% CIs were calculated based on the mean SWS ($k = 2$) of the first elastogram for each site, from both raters 1 and 2, using an absolute agreement, two-way random effects model. Test−retest reliability was calculated using the mean SWS of the first elastogram of each site at the two different time points. The ICC estimates and their 95% CIs were calculated using an absolute agreement, two-way mixed effects model.

The following analyses were conducted using the mean SWS of the first elastogram of each site, taken by rater 1, as the intra-rater reliability was excellent (detailed in results), indicating only one measurement was required. Descriptive statistics were used to calculate the mean and standard deviation of scars and controls. Boxplots were used to compare the median SWSs of controls with those of scars. The velocity data were inversely transformed to approximate a normal distribution; then linear regression and back transformation were used to estimate the difference in mean velocity between scars and controls.

Boxplots were used to evaluate the median SWS between the different VSS Height and VSS Pliability categories. To determine if there was an association between SWS and VSS scores two separate linear regression models were developed, one for VSS height and one for VSS pliability. The transformed SWS data were used as the independent variable and the VSS scores were the dependent variables in each model. A VSS score of 1 was used as the reference value to determine if the predicted mean SWSs were associated with each of the VSS categories and controls. Back-transformation to the original scale was conducted to calculate the predicted mean and standard errors.

Receiver operating characteristic (ROC) curve analysis was used to estimate the optimal SWS cutoff value that might be able to discriminate between normal skin, scars and pathologic scars. ROC curves were constructed for controls/scars, VSS Height score 1 and VSS Pliability score 1. The areas under the curves (AUCs) were evaluated, and the SWS value was chosen by maximizing the Youden index ($J = \text{sensitivity} + \text{specificity} - 1$), which maximizes the sensitivity and specificity (Thompson et al. 2015).

To assess if SWE could be used to estimate scar severity, the correlations between mean SWS and the VSS height score and the VSS pliability score were evaluated with Spearman's rank correlation coefficient. Spearman r values between 0.9 and 1 (−0.9 to −1) indicate a very high correlation, those from 0.7 to 0.9 (−0.7 to −0.9) a high correlation, those from 0.5 to 0.7 (−0.5 to −0.7) a moderate correlation and those below 0.5 (above −0.5) a low correlation (Mukaka 2012).

RESULTS

Fifty-five participants were recruited for this study, providing a total of 96 scars and 69 contralateral controls. The first 20 participants were excluded from statistical analysis because of the initial issues experienced with inconsistent imaging and the subsequent modifications made to the standoff and imaging protocol. Table 3 outlines the demographic characteristics of the remaining 35 participants, which included 61 scar sites, 45 (74%) of which were hypertrophic (VSS score ≥1), and 50 control sites. All scars resulted from a burn injury.

Table 4 details all the ICC results. In summary, excellent reliability (ICC > 0.93) was achieved for intra-rater, inter-rater and test−retest reliability of scars and normal skin combined. The reliability for scars and normal skin separately were excellent for both intra-rater and inter-rater reliability (ICC > 0.97). Test−retest reliability was good for scars (ICC > 0.85) and normal skin (ICC > 0.89).

Scars were on average 0.8 m/s stiffer than controls (95% CI: 0.5−1.01, $p < 0.001$). Table 5 summarizes the means, standard deviations and ranges of SWS for scars and controls. Boxplots (Fig. 3) highlight the differences in the medians between scars and controls. A number of outliers were noted in the boxplots; however, it was decided to keep them within the analysis as they may represent significant clinical information. Boxplots were

Table 3. Demographic details of participants in the reliability study

Demographic	Total recruited
No. of participants (scars/controls)	35 (61/50)
Pathologic scar defined as VSS ≥1	45 (74%)
Gender: male/female	20/15 (43%/57%)
Scar location, n (%)	
Upper arm	6 (10%)
Lower arm	9 (15%)
Wrist/hand	6 (10%)
Thigh	14 (23%)
Calf	9 (15%)
Shin	2 (3%)
Ankle/foot	10 (16%)
Chest	2 (3%)
Back	1 (2%)
Abdomen	2 (3%)
Months post-injury, mean (range)	11 (1−39)
Days between TP1 and TP2, mean (range)	5 (1−9)
Age, mean (range)	40 (19−73)
% TBSA, mean (range)	7% (0.25%−30%)

TBSA = total body surface area of the scar; TP = time point; VSS = Vancouver Scar Scale.

Table 4. Intra-class correlation coefficients for evaluating the reliability of shear wave speed

Intra-rater reliability

	Rater 1 No. of sites	Rater 1 ICC (95% CI), *p* value
Scars	100	0.98 (0.97−0.98), $p < 0.001$
Normal skin	81	0.98 (0.98−0.99), $p < 0.001$
Combined	181	0.98 (0.98−0.99), $p < 0.001$
	Rater 2 No. of sites	Rater 2 ICC (95% CI), *p* value
Scars	44	0.98 (0.98−0.99), $p < 0.001$
Normal skin	35	0.99 (0.99−0.99), $p < 0.001$
Combined	79	0.99 (0.98−0.99), $p < 0.001$

Inter-rater reliability

	No. of sites	ICC (95% CI), *p* value
Scars	44	0.94 (0.89−0.97), $p < 0.001$
Normal skin	35	0.98 (0.96−0.99), $p < 0.001$
Combined	79	0.96 (0.93−0.97), $p < 0.001$

Test-retest reliability

	No. of sites	ICC (95% CI), *p* value
Scars	40	0.92 (0.85−0.96), $p < 0.001$
Normal skin	31	0.88 (0.76−0.95), $p < 0.001$
Combined	71	0.93 (0.89−0.96), $p < 0.001$

CI = confidence interval; ICC = intra-class correlation coefficient.

constructed to compare the median SWSs of controls with the SWSs of scars separated into the VSS Height (Fig. 4) and VSS Pliability categories (Fig. 5).

A trend of increasing SWS with increasing VSS Height was observed, with an average increase of 2.3 m/s (95% CI: 2.1−2.5) in velocity with each increasing level of VSS Height. Predicted mean differences in velocity for each VSS Height are outlined in Table 6. No significant differences were noted in the SWS between flat scars and controls and between flat scars and scars raised >4 mm; however, only three scars in the study were >4 mm.

A trend of increasing SWS with increasing VSS Pliability scores was also observed. On average, the mean SWS increased 2.3 m/s (95% CI: 2.1−2.4) with each level of the VSS Pliability score. When each VSS Pliability level was compared, both yielding ($p = 0.002$) and firm ($p < 0.001$) scars were found to have increased velocity compared with normal scars (Table 6). Supple, banding and contracted scars did not significantly differ from scars with normal pliability in our small sample size.

ROC analysis (Fig. 6) revealed that the optimal cutoff point for discriminating hypertrophic scars (VSS Height score ≥1) from flat scars and controls was 2.22 m/s (14.48 kPa), with 71% sensitivity, 82% specificity and an AUC of 0.82. The optimal cutoff SWS for discriminating clinically assessed reduced pliability (VSS Pliability score ≥1) was also 2.22 m/s (14.48 kPa), with a 70% sensitivity, 88% specificity and AUC of 0.82. The optimal cutoff SWS for discriminating scars from controls was 2.09 m/s (13.1 kPa) with a 70% sensitivity, 76% specificity and AUC of 0.78.

Spearman's rho between mean SWS and VSS Pliability was 0.66 ($p < 0.001$), and that between mean SWS and VSS Height was 0.47 ($p < 0.001$).

Subjectively it was observed that in some instances, tissues below the scar, including the subcutaneous adipose, fascia and muscle, exhibited increased stiffness, which was not seen in the control tissue (Fig. 7).

DISCUSSION

This study developed a reliable, novel protocol to evaluate the stiffness of burn scars using SWE. The protocol had excellent intra-rater reliability for both the novice clinician and the experienced sonographer and excellent inter-rater reliability between the two. These

Table 5. Shear-wave speed and shear modulus of controls and scars

Scar Vancouver Scar Score	Number	Shear wave Speed (m/s) Mean (SD), range	Shear modulus (kPa) Mean (SD), range
Controls	50	1.93 (0.74), 1.06−4.94	12.93 (12.57), 3.4−73.5
Scars (overall)	61	3.13 (1.63), 1.25−9.37	38.49 (46.46), 4.72−265.51
VSS scar height			
0: Flat scar	16	2.27 (0.93), 1.25−4.48	18.20 (16.41), 4.72−61.04
1: 0−1 mm	19	2.83 (1.15), 1.63−5.65	28.79 (26.05), 8.24−97.23
2: 1−2 mm	16	3.44 (1.48), 1.45−5.91	43.11 (33.17), 6.56−107.92
3: 2−4 mm	7	4.65 (2.99), 2.17−9.37	90.36 (105.54), 14.26−265.51
4: >4 mm	3	4.41 (0.51), 4.09−5.01	62.35 (18.05), 51.05−83.17
VSS scar pliability			
0: "normal" scar	8	1.82 (0.31), 1.25−2.19	10.29 (3.31), 4.72−14.59
1: Supple	13	2.03 (0.54), 1.56−3.29	13.44 (7.68), 7.42−32.73
2: Yielding	14	3.10 (0.93), 1.42−4.31	31.93 (17.70), 6.56−56.71
3: Firm	24	4.12 (1.97), 1.89−9.37	64.43 (63.37), 10.89−265.51
4: Banding	1	3.01	28.48
5: Contracture	1	4.68	68.64

SD = standard deviation; VSS = Vancouver Scar Scale.

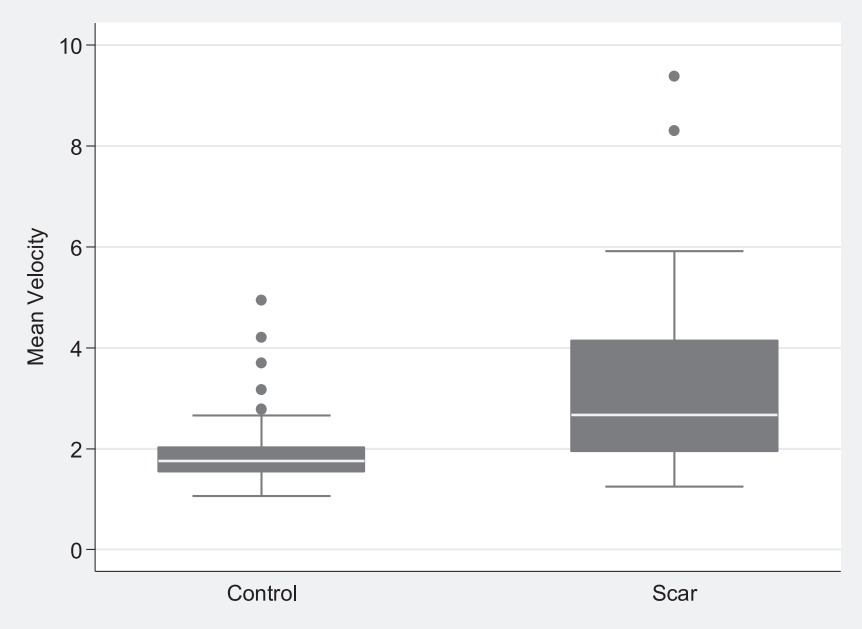

Fig. 3. Boxplot revealing the difference between the shear wave speeds of scars and controls.

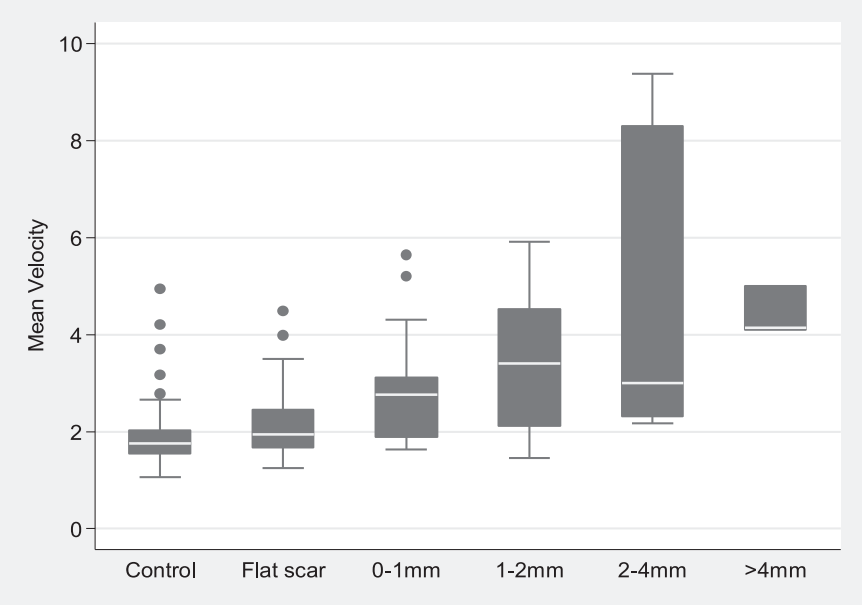

Fig. 4. Boxplot of the shear wave speeds of controls and scars separated into Vancouver Scar Scale Height score categories.

results indicate that the level of training (10 h) received by the novice was adequate to acquire images. In addition, the excellent test–retest reliability indicates that SWE is suitable for longitudinal studies and repeat clinical scar evaluation.

Overall, burn scars were significantly stiffer than controls, with preliminary SWS cutoff values identified to discriminate between normal skin, non-pathologic scars and pathologic scars. Although hypertrophic scarring is the most common form of pathologic scarring reported after a burn, the classification of what constitutes a hypertrophic scar is ill-defined and a source of debate (Thompson et al. 2015). Recent research suggested a raised scar scoring $\geq$1 in VSS Height was the most accurate method of classification (Thompson et al. 2015). The results of the present study support this

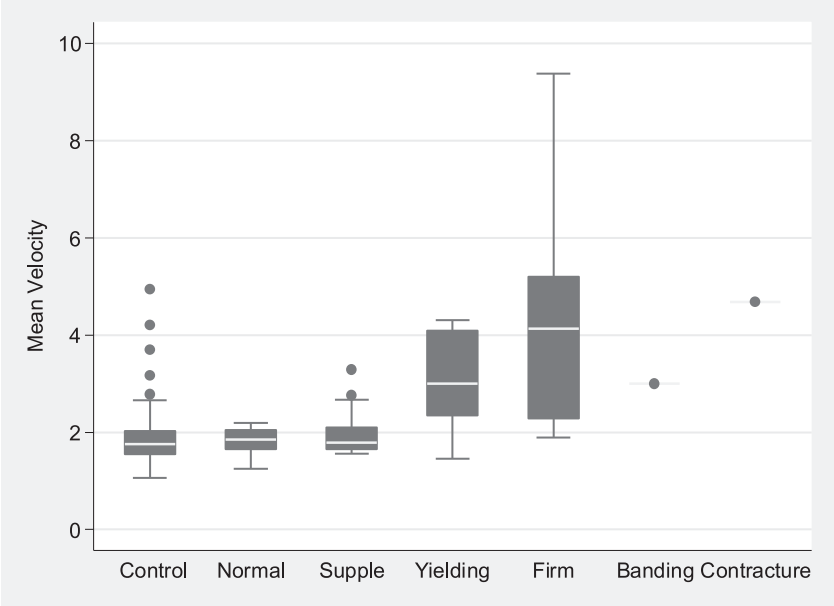

Fig. 5. Boxplot of the shear wave speeds of controls and scars separated into Vancouver Scar Scale Pliability score categories.

Table 6. Predicted difference in mean SWS between the VSS scores

	N	Predicted difference in mean SWS (m/s)	95% CI	*p* Value
VSS Height				
Control	50	−0.27	−0.60 to 0.06	0.112
Flat scar	16	Reference	—	—
0−1 mm	19	0.47	−0.05 to 0.99	0.077
1−2 mm	16	0.83	0.16−1.51	0.016
2−4 mm	4	1.42	0.05−2.79	0.042
>4 mm	3	2.36	−0.96 to 5.68	0.163
VSS Pliability				
Control skin	50	−0.02	−0.35 to 0.31	0.909
Normal scar	8	Reference	—	—
Supple	13	0.16	−0.26 to 0.58	0.445
Yielding	14	1.04	0.38−1.70	0.002
Firm	24	1.60	0.89−2.31	<0.001
Banding	1	1.24	−1.28 to 3.76	0.335
Contracture	1	2.92	−3.16 to 9.00	0.347

CI = confidence interval; SWS = shear wave speed; VSS = Vancouver Scar Scale.

recommendation, suggesting that there is no significant difference in stiffness between flat scars (VSS Height = 0) and controls, but significant differences in stiffness between flat scars and raised scars. Although a statistical difference was not found between flat scars and scars raised >4 mm, this was possibly owing to the small sample size of 3 in this group.

Both the VSS Height ≥1 and Pliability ≥1 scores produced the same SWS cutoff score of 2.22 m/s (14.48 kPa) for pathologic scars. Scar height and pliability are often correlated (Wallace et al. 2019); however, they can change independently of each other over the course of scar formation (Lee et al. 2016). Results of this study indicate that only 50% of flat (non-pathologic) scars also had normal pliability as assessed by the VSS (Table 5). Additionally, all scars with normal pliability had SWSs below the 2.22 m/s cutoff value, whereas a large range of SWSs (1.25−4.48 m/s) were noted in flat scars. These results suggest that some flat scars had pathologic levels of stiffness. However, there was also a wide range of SWSs in controls (1.06−4.94 m/s), which contributed to the lower than desired sensitivity and specificity of the SWS cutoff values. Similarly, Yang et al. (2019) evaluated 60 healthy controls with SWE and also had a wide range of shear modulus measurements for normal skin ranging from 6.9 kPa in the abdomen to 43.8 kPa on the dorsal middle phalanx of the finger. Skin stiffness is known to vary with a number of variables including different body locations (Hou et al. 2015; Wang et al. 2019; Yang et al. 2018, 2019), sex (Yang et al. 2018) and age (Pawlaczyk et al. 2013), which were not accounted for in our analysis. These factors may influence the clinical interpretation of SWS and the diagnosis of pathologic scars based on SWS levels. Further studies evaluating the relative difference between matched scars and controls and powered to account for patient variables are recommended to further evaluate the preliminary cutoff values obtained in this study.

Both increasing scar height and increasing pliability scores were associated with increasing SWS, as assessed with the regression models. This, together with the moderate Spearman correlation between SWS and VSS

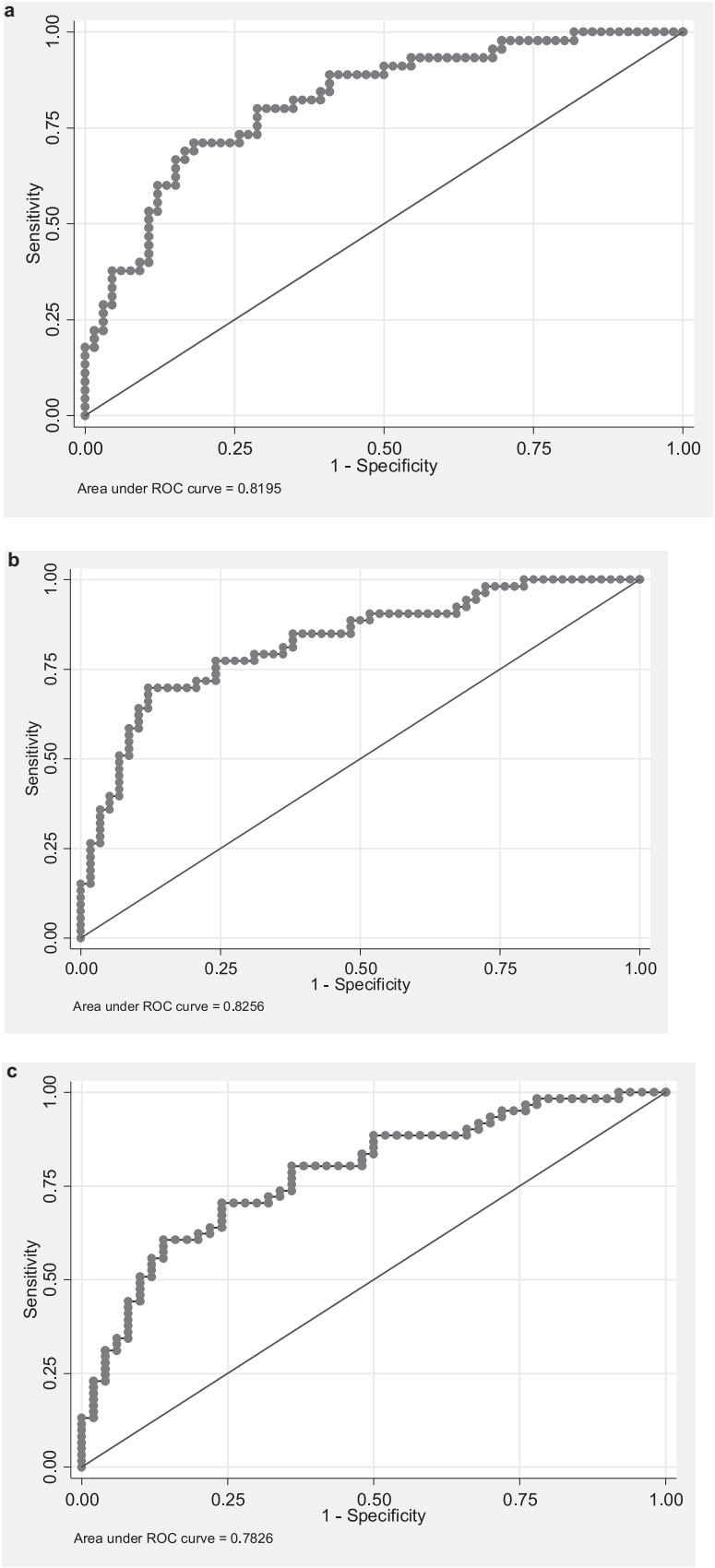

Fig. 6. Reciever operating characteristic (ROC) curves. (a) ROC curve for determining the cutoff shear wave speed (SWS) for scars with a Vancouver Scar Scale Height score ≥1. (b) ROC curve for determining the cutoff SWS for scars with a Vancouver Scar Scale Pliability score ≥1. (c) ROC curve for determining the SWS cutoff for controls.

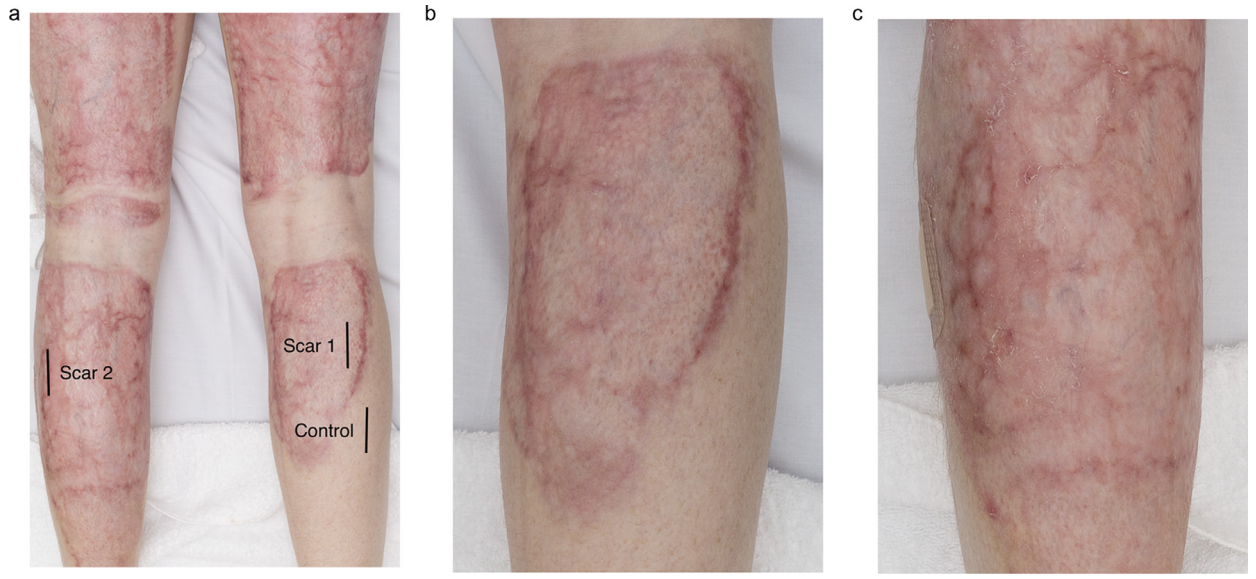

Fig. 7. Elastograms revealing increased stiffness of underlying tissues. Elastograms of three different sites on the calves of a 35-y-old woman, 6 mo after flame burns to her lower legs. (a) Photograph of both calves= depicting the three points of assessment. (b) Closeup of scar 1, a deep partial-thickness burn on the right calf with a resulting flat (Vancouver Scar Scale [VSS] Height = 0) and supple (VSS Pliability = 1) scar. (c) Closeup of scar 2, a deep partial-thickness burn on her left calf with a slightly raised (VSS Height = 1) and firm (VSS Pliability = 3) scar. (d) Elastograpm of the control on her right calf. (e) Elastogram of scar 1. (f) Elastogram of scar 2. Note the progressive increase in stiffness of the skin and subcutaneous tissues with increasing VSS Pliability scores, including increased stiffness of the adipose tissue, deep fascia and muscle. subcut = subcutaneous adipose tissue.

Pliability ($r = 0.65$), suggests that SWE has the potential to quantify the severity of scar stiffness. Hypertrophic scars slowly increase in stiffness over the first 6−12 mo, then slowly regresses over the next ≥2 y (Nedelec et al. 2014; Ghazawi et al. 2018). Non-pathologic scars, on the other hand, may exhibit early induration, with the stiffness decreasing to normal levels by 1−3 mo post-injury. The ability to monitor the severity of scar stiffness over time is essential for developing a better understanding of the different trajectories of pathologic and non-pathologic scar formation and for evaluating treatment efficacy at various time points. Scar pliability at 3 mo post-injury can predict scar quality at 18 mo post-injury (Goei et al. 2017). However, scars are well established at 3 mo; therefore, SWE may provide an opportunity to develop earlier indictors of pathologic scarring, so earlier intervention can be implemented. Further research is recommended to investigate changes in scar SWS over time and investigate the minimal detectable differences and clinically meaningful differences to further define scar severity.

The VSS Pliability linear regression model revealed that only scars with a VSS Pliability score of 2 or 3 had SWSs that were significantly different from those of scars with normal pliability, whereas scars with a VSS Pliability score of 1, 4 and 5 were not significantly different. Although the small sample size could explain this finding, another explanation may relate to increased stiffness of tissues underlying the scar (subcutaneous adipose, deep fascia and/or muscle), which was observed in a number of scar elastograms. Long-term sequelae of a burn injury include reduced range of movement, contracture (Oosterwijk et al. 2017; Schouten et al. 2019) and musculoskeletal disorders (Barrett et al. 2019), which can relate to tight, stiff underlying tissue. Increased stiffness of underlying tissues may influence the clinician's perception of the palpable "skin" stiffness, which may not have been captured by only taking SWS measurements of the skin. However, another possibility is that the increased stiffness of underlying tissue may generate artifactual SWS in the skin. Increased SWSs have been recorded in skin located in close proximity to the underlying bone, which could be owing to high signal reflection off the bone (Hou et al. 2015; Sun et al. 2017). Further research is recommended to investigate the effects of underlying tissue stiffness on SWS in the skin and the potential use for evaluating the mechanical changes associated with non-injured tissues deep to the dermal burn.

A strength of this study was the heterogeneous sample of burn scars ranging from flat and pliable to raised and stiff scars so the capacity of SWE to discriminate between a range of scar severities could be assessed.

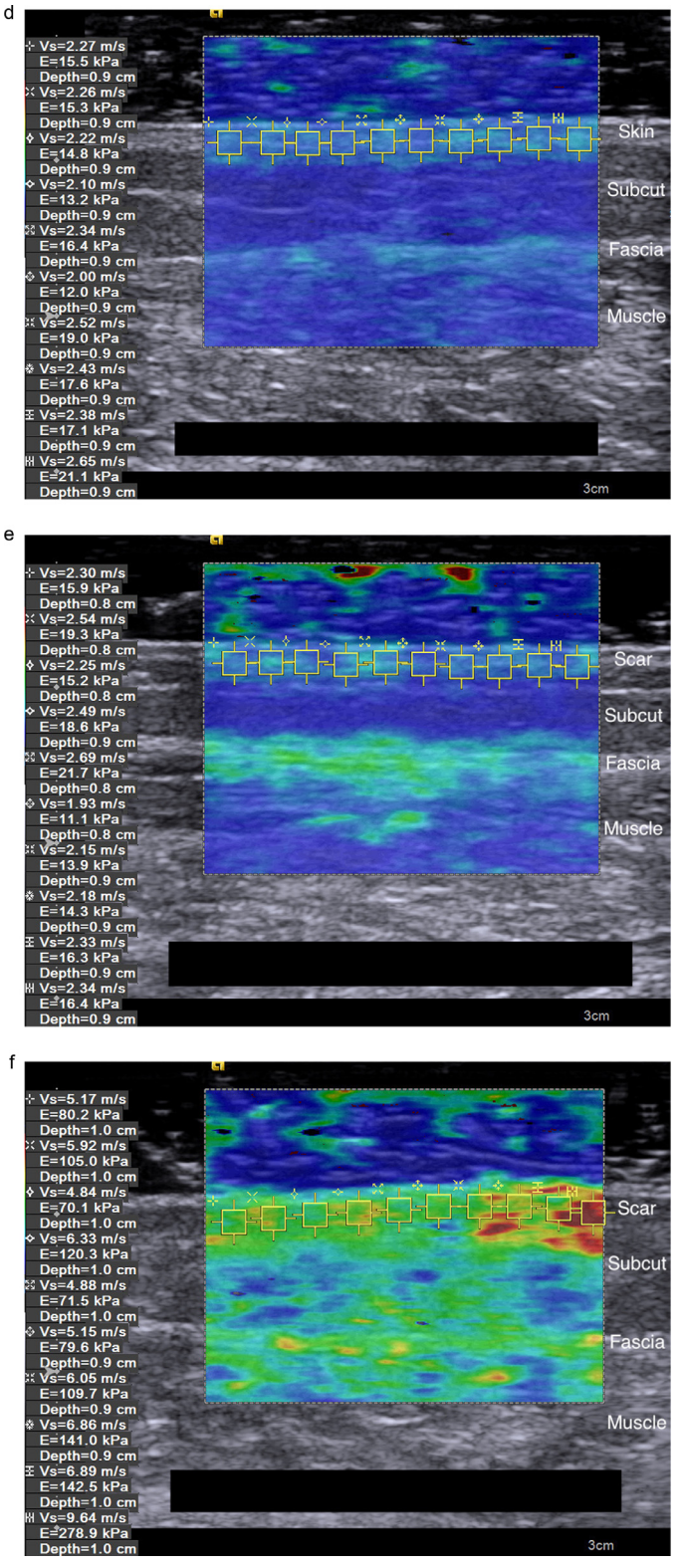

Fig. 7. Continued

Prior objective scar assessment tools have had a limited capacity to evaluate severe scars such as those with increased stiffness and/or increased height (Nedelec et al. 2008; Gankande et al. 2014), whereas SWE had the ability to reliably evaluate scars of severe stiffness and height. Further research on larger samples and a variety of scars is recommended to confirm our results.

A limitation of our study was the use of SWS rather than shear modulus in our analysis; therefore, the results of our study cannot be generalized. The shear modulus is a physiologic parameter that can be used for comparing studies and developing normative data. The shear modulus is an estimate based on the measured SWS; however, the algorithms used to calculate the shear modulus from the SWS have not, to our knowledge, been validated for use in dermatology. Different elastography systems have different capabilities and, when evaluated under similar conditions, produce different SWSs (Dillman et al. 2015; Shin et al. 2016; Zelesco et al. 2018). Therefore, further studies are required to ensure shear modulus conversion is accurate for use in dermatology and is comparable among the different commercial systems.

Elastography of skin and scar tissue is still in its infancy and during the time span of this study, elastography probes using an 18-MHz frequency were developed. These may improve evaluation of cutaneous conditions. Studies assessing the impact of imaging depth, coupling medium and probe frequency, both *in vivo* and on skin-mimicking phantoms, may be merited. These data may lead to improved study protocols addressing image optimization and accurate shear modulus measurements. The initial difficulties experienced obtaining reproducible images with standard imaging protocols have highlighted the need to evaluate protocol reliability before conducting clinical studies and the need for collaborative development of recommended imaging protocols in dermatology to ensure high standards in practice are adopted.

CONCLUSIONS

This pilot study developed a reliable, novel protocol to evaluate skin and burn scar stiffness using SWE with a 9-MHz probe. Preliminary results suggest that SWE is able to discriminate between scars and normal skin and has the ability to evaluate scar severity. Larger studies are required to evaluate how patient factors (*e.g.,* age, sex and body location) influence both the measured velocity and the clinical interpretation of velocity values. The development of an objective, non-invasive method to quantify scar stiffness is essential to improve point-of-care assessment, detect early signs of pathologic scarring, evaluate treatment efficacy and advance research investigating the mechanical mechanisms underlying scar formation. Shear wave elastography shows great potential for filling this gap. Further development of the technology to optimize imaging for superficial tissues would advance the incorporation of this technology into standard clinical care.

Acknowledgments—We acknowledge and thank all the patients that took the time to participate in this study, and the staff at the Burns Outpatient Clinic at Fiona Stanley Hospital that assisted and supported this research.

Conflict of interest disclosure—Siemens Heathineers provided the S3000 system for the use of this research. However, the company was not involved in the design or conduction of this research, nor did they have the opportunity to edit or review this article before publication.

B.K. is a founder and shareholder in OncoRes Medical (Perth, Western Australia, Australia), a start-up company developing optical-based elastography for surgical applications. In addition, he performs funded research for this company.

REFERENCES

Aya R, Yamawaki S, Muneuchi G, Naitoh M, Suzuki S. Ultrasound elastography to evaluate keloids. Plast Reconstr Surg Glob Open 2014;2(2):e106.

Aya R, Yamawaki S, Yoshikawa K, Katayama Y, Enoshiri T, Naitoh M, Suzuki S. The shear wave velocity on elastography correlates with the clinical symptoms and histopathological features of keloids. Plast Reconstr Surg Glob Open 2015;3(7):e464.

Bamber J, Cosgrove D, Dietrich C, Fromageau J, Bojunga J, Calliada F, Cantisani V, Correas J-M, D'onofrio M, Drakonaki E. EFSUMB guidelines and recommendations on the clinical use of ultrasound elastography: Part 1. Basic principles and technology. Ultraschall Med 2013;34:169–184.

Barr RG, Nakashima K, Amy D, Cosgrove D, Farrokh A, Schafer F, Bamber JC, Castera L, Choi BI, Chou YH. WFUMB guidelines and recommendations for clinical use of ultrasound elastography: Part 2. Breast. Ultrasound Med Biol 2015;41:1148–1160.

Barrett LW, Fear VS, Waithman JC, Wood FM, Fear MW. Understanding acute burn injury as a chronic disease. Burns Trauma 2019;7:23.

Baryza M, Baryza G. The Vancouver Scar Scale: An administration tool and its interrater reliability. J Burn Care Rehabil 1995;16:535–538.

Bhatia KS, Cho CC, Tong CS, Yuen EH, Ahuja AT. Shear wave elasticity imaging of cervical lymph nodes. Ultrasound Med Biol 2012a;38(2):195–201.

Bhatia KS, Yuen EH, Cho CC, Tong CS, Lee YY, Ahuja AT. A pilot study evaluating real-time shear wave ultrasound elastography of miscellaneous non-nodal neck masses in a routine head and neck ultrasound clinic. Ultrasound Med Biol 2012b;38(6):933–942.

Botar-Jid CM, Cosgarea R, Bolboacă SD, Şenilă SC, Lenghel LM, Rogojan L, Dudea SM. Assessment of cutaneous melanoma by use of very-high-frequency ultrasound and real-time elastography. AJR Am J Roentgenol 2016;206(4):699–704.

Browne AL, Andrews R, Schug SA, Wood F. Persistent pain outcomes and patient satisfaction with pain management after burn injury. Clin J Pain 2011;27:136–145.

Cannaò PM, Vinci V, Caviggioli F, Klinger M, Orlandi D, Sardanelli F, . . ., Sconfienza LM. Technical feasibility of real-time elastography to assess the peri-oral region in patients affected by systemic sclerosis. J Ultrasound 2014;17(4):265–269.

Chang S, Kim M-J, Kim J, Lee M-J. Variability of shear wave velocity using different frequencies in acoustic radiation force impulse (ARFI) elastography: a phantom and normal liver study. Ultraschall Med 2013;34(03):260–265.

Creze M, Nordez A, Soubeyrand M, Rocher L, Maître X, Bellin MF. Shear wave sonoelastography of skeletal muscle: Basic principles, biomechanical concepts, clinical applications, and future perspectives. Skeletal Radiol 2018;47:457–471.

DeJong HM, Abbott S, Zelesco M, Kennedy BF, Ziman MR, Wood FM. The validity and reliability of using ultrasound elastography to

measure cutaneous stiffness, a systematic review. Int J Burns Trauma 2017a;7:124.
DeJong HM, Phillips M, Edgar DW, Wood FM. Patient opinion of scarring is multidimensional: An investigation of the POSAS with confirmatory factor analysis. Burns 2017b;43:58–68.
Dietrich C, Bamber J, Berzigotti A, Bota S, Cantisani V, Castera L, Cosgrove D, Ferraioli G, Friedrich-Rust M, Gilja O, Goertz RS, Karlas T, de Knegt R, de Ledinghen V, Piscaglia F, Procopet B, Saftoiu A, Sidhu PS, Sporea I, Thiele M. EFSUMB guidelines and recommendations on the clinical use of liver ultrasound elastography, update 2017 (long version). Ultraschall Med 2017;38:e16–e47.
Dillman JR, Chen S, Davenport MS, Zhao H, Urban MW, Song P, ..., Carson PL. Superficial ultrasound shear wave speed measurements in soft and hard elasticity phantoms: repeatability and reproducibility using two ultrasound systems. Pediatric Radiology 2015;45(3):376–385.
Duke J, Rea S, Semmens J, Edgar DW, Wood F. Burn and cancer risk: A state-wide longitudinal analysis. Burns 2012;38:340–347.
Duke JM, Bauer J, Fear MW, Rea S, Wood FM, Boyd J. Burn injury, gender and cancer risk: Population-based cohort study using data from Scotland and Western Australia. BMJ Open 2014;4: e003845.
Fear M, Wood F. The role of big data in burns care of the future. J Burn Care Res 2018;39:S239.
Ferguson MW, healing O'Kane SScar−free. From embryonic mechanisms to adult therapeutic intervention. Philos Trans R Soc Lond B Biol Sci 2004;359:839–850.
Ferraioli G, Filice C, Castera L, Choi BI, Sporea I, Wilson SR, Cosgrove D, Dietrich CF, Amy D, Bamber JC. WFUMB guidelines and recommendations for clinical use of ultrasound elastography: Part 3. Liver. Ultrasound Med Biol 2015;41:1161–1179.
Gankande T, Wood F, Edgar D, Duke J, DeJong H, Henderson A, Wallace H. A modified Vancouver Scar Scale linked with TBSA (mVSS-TBSA): Inter-rater reliability of an innovative burn scar assessment method. Burns 2013;39:1142–1149.
Gankande T, Duke J, Danielsen P, DeJong H, Wood F, Wallace H. Reliability of scar assessments performed with an integrated skin testing device—The DermaLab Combo®. Burns 2014;40:1521–1529.
Ghazawi FM, Zargham R, Gilardino MS, Sasseville D, Jafarian F. Insights into the pathophysiology of hypertrophic scars and keloids: How do they differ? Adv Skin Wound Care 2018;31:582–595.
Goei H, van der Vlies C, Tuinebreijer W, van Zuijlen P, Middelkoop E, van Baar M. Predictive validity of short term scar quality on final burn scar outcome using the Patient and Observer Scar Assessment Scale in patients with minor to moderate burn severity. Burns 2017;43:715–723.
Hesselstrand R, Scheja A, Wildt M, Åkesson A. High-frequency ultrasound of skin involvement in systemic sclerosis reflects oedema, extension and severity in early disease. Rheumatology 2008;47:84–87.
Hinz B. The extracellular matrix and transforming growth factor-β1: Tale of a strained relationship. Matrix Biol 2015;47:54–65.
Hou Y, Zhu QL, Liu H, Jiang YX, Wang L, Xu D, Li MT, Zeng XF, Zhang FC. A preliminary study of acoustic radiation force impulse quantification for the assessment of skin in diffuse cutaneous systemic sclerosis. J Rheumatol 2015;42:449–455.
Hu H, Zhu X, Wang C, Zhang L, Li X, Lee S, ..., Wang C. Stretchable ultrasonic transducer arrays for three-dimensional imaging on complex surfaces. Sci Adv 2018;4(3): eaar3979.
Kallini JR, Hamed N, Khachemoune A. Squamous cell carcinoma of the skin: Epidemiology, classification, management, and novel trends. Int J Dermatol 2015;2:130–140.
Koo TK, Li MY. A guideline of selecting and reporting intraclass correlation coefficients for reliability research. J Chiropr Med 2016;15:155–163.
Lee SY, Cardones AR, Doherty J, Nightingale K, Palmeri M. Preliminary results on the feasibility of using ARFI/SWEI to assess cutaneous sclerotic diseases. Ultrasound Med Biol 2015;41:2806–2819.
Lee KC, Dretzke J, Grover L, Logan A, Moiemen N. A systematic review of objective burn scar measurements. Burns Trauma 2016;4:14.
Li J, Li-Tsang CW, Huang Y, Chen Y, Zheng Y. Detection of changes of scar thickness under mechanical loading using ultrasonic measurement. Burns 2013;39:89–97.
Liu K, Bhatia K, Chu W, He L, Leung S, Ahuja A. Shear wave elastography–a new quantitative assessment of post-irradiation neck fibrosis. Ultraschall Med 2015;36(04):348–354.
Luo CC, Qian LX, Li GY, Jiang Y, Liang S, Cao Y. Determining the in vivo elastic properties of dermis layer of human skin using the supersonic shear imaging technique and inverse analysis. Med Phys 2015;42:4106–4115.
Mandava A, Ravuri PR, Konathan R. High-resolution ultrasound imaging of cutaneous lesions. Indian J Radiol Imaging 2013;23:269.
Morris M, Ring C, Managuli R, Saboury B, Mehregan D, Siegel E, Dasgeb B. Feature analysis of ultrasound elastography image for quantitative assessment of cutaneous carcinoma. Skin Res Technol 2018;24(2):242–247.
Mukaka MM. A guide to appropriate use of correlation coefficient in medical research. Malawi Med J 2012;24:69–71.
Nedelec B, Correa J, Rachelska G, Armour A, LaSalle L. Quantitative measurement of hypertrophic scar: Interrater reliability and concurrent validity. J Burn Care Res 2008;29:501–511.
Nedelec B, Correa JA, de Oliveira A, LaSalle L, Perrault I. Longitudinal burn scar quantification. Burns 2014;40:1504–1512.
O'Hara S, Zelesco M, Rocke K, Stevenson G, Sun Z. Reliability indicators for 2−dimensional shear wave elastography. J Ultrasound Med 2019;38:3065–3071.
Oosterwijk AM, Mouton LJ, Schouten H, Disseldorp LM, van der Schans CP, Nieuwenhuis MK. Prevalence of scar contractures after burn: A systematic review. Burns 2017;43:41–49.
Ophir J, Cespedes I, Ponnekanti H, Yazdi Y, Li X. Elastography: A Quantitative method for imaging the elasticity of biological tissues. Ultrason Imaging 1991;13:111–134.
Palmeri ML, Qiang B, Chen S, Urban MW. Guidelines for finite-element modeling of acoustic radiation force-induced shear wave propagation in tissue-mimicking media. IEEE Trans Ultrason Ferroelectr Freq Control 2017;64(1):78–92.
Pawlaczyk M, Lelonkiewicz M, Wieczorowski M. Age-dependent biomechanical properties of the skin. Adv Dermatol Allergol 2013;30:302.
Săftoiu A, Gilja OH, Sidhu PS, Dietrich CF, Cantisani V, Amy D, Bachmann-Nielsen M, Bob F, Bojunga J, Brock M. The EFSUMB guidelines and recommendations for the clinical practice of elastography in non-hepatic applications: Update 2018. Ultraschall Med 2019;40:425–453.
Santiago T, Alcacer-Pitarch B, Salvador M, Del Galdo F, Redmond A, da Silva J. A preliminary study using Virtual Touch imaging and quantification for the assessment of skin stiffness in systemic sclerosis. Clin Exp Rheumatol 2016;34:S137–S141.
Sarvazyan AP, Rudenko OV, Swanson SD, Fowlkes JB, Emelianov SY. Shear wave elasticity imaging: A new ultrasonic technology of medical diagnostics. Ultrasound Med Biol 1998;24:1419–1435.
Schouten H, Nieuwenhuis M, van Baar M, van der Schans C, Niemeijer A, van Zuijlen P. The prevalence and development of burn scar contractures: A prospective multicenter cohort study. Burns 2019;45:783–790.
Shin HJ, Kim M-J, Kim HY, Roh YH, Lee M-J. Comparison of shear wave velocities on ultrasound elastography between different machines, transducers, and acquisition depths: a phantom study. Eur Radiol 2016;26(10):3361–3367.
Simons M, Kee EG, Kimble R, Tyack Z. Ultrasound is a reproducible and valid tool for measuring scar height in children with burn scars: A cross-sectional study of the psychometric properties and utility of the ultrasound and 3D camera. Burns 2017;43:993–1001.
Sun Y, Ma C, Liang X, Wang R, Fu Y, Wang S, Cui L, Zhang C. Reproducibility analysis on shear wave elastography (SWE)-based quantitative assessment for skin elasticity. Medicine 2017;96:e6902.
Thompson CM, Sood RF, Honari S, Carrougher GJ, Gibran NS. What score on the Vancouver Scar Scale constitutes a hypertrophic scar? Results from a survey of North American burn-care providers. Burns 2015;41:1442–1448.
Trevethan R. Intraclass correlation coefficients: Clearing the air, extending some cautions, and making some requests. Health Serv Outcomes Res Method 2017;17:127–143.

van der Wal MB, Tuinebreijer WE, Lundgren-Nilsson A, Middelkoop E, van Zuijlen PP. Differential item functioning in the Observer Scale of the POSAS for different scar types. Qual Life Res 2014;23:2037–2045.

Wallace HJ, Cadby G, Melton PE, Wood FM, Falder S, Crowe MM, Martin LJ, Marlow K, Ward SV, Fear MW. Genetic influence on scar height and pliability after burn injury in individuals of European ancestry: A prospective cohort study. Burns 2019;45:567–578.

Walraven M, Hinz B. Therapeutic approaches to control tissue repair and fibrosis: Extracellular matrix as a game changer. Matrix Biology 2018;71/72:205–224.

Wang XQ, Mill J, Kravchuk O, Kimble RM. Ultrasound assessed thickness of burn scars in association with laser Doppler imaging determined depth of burns in paediatric patients. Burns 2010;36:1254–1262.

Wang L, Yan F, Yang Y, Xiang X, Qiu L. Quantitative assessment of skin stiffness in localized scleroderma using ultrasound shear-wave elastography. Ultrasound Med Biol 2017;43:1339–1347.

Wang Y, Shan JL, Chen HY, Wu ZF. Comparison of 2−D shear wave elastography with clinical score in localized scleroderma: A new method to increase the diagnostic accuracy. J Dermatol 2019;46:131–138.

Wortsman X. Atlas of dermatologic ultrasound. Berlin/New York: Springer, 2018:35−83.

Xiang X, Yan F, Yang Y, Tang Y, Wang L, Zeng J, Qiu L. Quantitative assessment of healthy skin elasticity: Reliability and feasibility of shear wave elastography. Ultrasound Med Biol 2017;43:445–452.

Yang Y, Wang L, Yan F, Xiang X, Tang Y, Zhang L, Liu J, Qiu L. Determination of normal skin elasticity by using real−time shear wave elastography. J Ultrasound Med 2018;37:2507–2516.

Yang Y, Qiu L, Wang L, Xiang X, Tang Y, Li H, Yan F. Quantitative assessment of skin stiffness using ultrasound shear wave elastography in systemic sclerosis. Ultrasound Med Biol 2019;45:902–912.

Zelesco M, Abbott S, O'hara S. Pitfalls and sources of variability in two dimensional shear wave elastography of the liver: An overview. Sonography 2018;5(1):20–28.